Variations in Sediment Strength along the Tidal Inlet Channel near Pea Island, NC

Reem Jaber[1], Nina Stark, Ph.D., M.ASCE[2], Anna Wargula, Ph.D. [3], Liliana Velásquez-Montoya, Ph.D. M. ASCE[4]., Elizabeth Sciaudone, Ph.D., P.E[5].

[1]200 Patton Hall, Department of Civil and Environmental Engineering, Virginia Tech. e-mail: reemj@vt.edu.
[2]200 Patton Hall, Department of Civil and Environmental Engineering, Virginia Tech. e-mail: ninas@vt.edu.
[2]346 Rickover Hall, Department of Naval Architecture and Ocean Engineering, U.S. Naval Academy. email: wargula@usna.edu.
[2]346 Rickover Hall, Department of Naval Architecture and Ocean Engineering, U.S. Naval Academy. email: velasque@usna.edu.
[3]313 Mann Hall, Department of Civil, Construction and Environmental Engineering, North Carolina State University. email:ejsciaud@ncsu.edu.

ABSTRACT

The sound-side shoreline of Pea Island located on the Outer Banks, NC has been eroding over the last two decades. As part of the During Nearshore Event Experiment (DUNEX) pilot experiment carried out in October 2019, sediment strength, grain size, and currents were measured in a tidal inlet flood channel in the back-barrier zone of Pea Island using a portable free fall penetrometer, grab samples, and an acoustic Doppler current profiler. Results indicate a general trend of a decrease in the surficial (upper 10 cm) sediment strength towards the shoreline (from ~130 kPa to ~75 kPa) and from downstream to upstream (from ~150 kPa to 70 kPa). The cross-shore directed trend can be explained by sediment fining towards the shoreline with a lowest median grain size of 22 μm. Variations in sediment strength were related to current velocities and local sediment transport processes; thus, the results contribute to a better understanding of the erosional processes of the sediments.

INTRODUCTION

The Outer Banks of North Carolina, shown in Figure 1a, is a chain of barrier islands extending along 320 km of the Atlantic Coast (Inman and Dolan, 1989). These barrier islands are known to be some of the most dynamic natural deposits systems and are subject to continuous change through various hydrodynamic conditions, being primarily waves, currents, and extreme events (Dolan and Lins 2000; Dolan et al. 2016). The Outer Banks formed naturally through a combination of sea level rise and sand supply accompanied by strong waves or winds (Dolan and Lins 2000). It has been reported that the islands have been migrating south and landward over the long term as a result of sediment transport processes and wave action (Riggs et al. 2009). Low-lying and narrow portions of these barrier islands are frequently breached due to dune erosion, and dune overtopping during extreme events (Clinch et al., 2012; Safak et al. 2016). Although these breaches can have a positive impact on ecosystems and provide sediments close to the shoreline, their effects can be devastating on coastal infrastructure (Castelle et al., 2007; Safak et al. 2016).

Pea Island is an approximately 20 km long "simple" barrier island along the chain of the Outer Banks islands. Simple barrier islands are characterized by low elevations due to the limited sediment supply, which makes them prone to overwash process and inlet formations (Riggs et al. 2009). Pea Island is subject to frequent inlet formations and closures due to extreme events (Velasquez-Montoya et al. 2018). However, Oregon Inlet, which opened during a hurricane in 1846, is the only remaining active inlet at Pea Island. Inlet sediment dynamics often make it difficult to maintain a safe navigational channel without human interventions such as dredging or jetty/groin construction. These interventions interfere with the natural sediment transport processes driving channel migration and impact shoreline erosion rates (Riggs et al. 2009). The continuous migration of the channel and breaches of the shoreline have destroyed parts of North Carolina Highway 12 (NC HWY 12) over the years. Migration of Oregon Inlet has threatened the structural stability of the bridge that crosses the inlet and raised concerns regarding the long-term stability plans of the coastal infrastructure.

NC HWY 12 is the only North-to-South route along the Outer Banks. This coastal infrastructure is at great risk of scour/erosion due to migration of both the ocean and estuarine shorelines and breaches during coastal storms (Sciaudone et al. 2016). This is aggravated by the dynamic nature of sound-side processes combined with the complex inlet processes (Seminack and McBride 2018) and raises concern on the ability to protect island infrastructure from future breaches and inlet-related processes, especially during extreme events (Sciaudone et al. 2016). Consequently, the North Carolina Department of Transportation (NCDOT) started a monitoring program of the island in 2010 to assess the vulnerability of the highway and to assist in the planning for future phases of NC HWY 12 (Velasquez-Montoya et al. *in press*).

The Outer Banks have been impacted by numerous hurricanes and extreme events, and Pea Island has sustained some of the most severe damage from extreme events (Dolan and Lins 2000; Velasquez-Montoya et al. 2018). The engineering attempts to ensure safe navigation at Pea Island has required continuous dredging, which has interfered in the island's natural dynamic processes leading to more narrowing of the island and susceptibility to future breaches (Riggs et al. 2009; Riggs and Ames 2011). These sediment transport disturbances have significantly altered the sediment budget and modified erosion rates along Pea Island shorelines (Inman and Dolan 1989; Riggs et al. 2009; Pietrafesa 2012). Erosion rates are also affected by the sediment type and geotechnical properties. Grain size is the oldest and most widely used parameter represented in erosion equations/models of coarse-grained sediments. Larger grain sizes are often linked with increased sediment resistance and cohesive sediments are harder to erode than sandy material (Grabowski et al. 2011). However, other geotechnical properties contribute to the sediment erodibility, especially in fine-grained sediments, such as grain size distribution, bulk density, Atterberg limits, shear strength and others (Grabowski et al. 2011).

Pea Island's susceptibility to coastal storms and the history of human interventions has attracted the attention of researchers to improve predictions of local sediment dynamics (Inman and Dolan 2000; Riggs et al. 2009; Dolan et al. 2016; Sciaudone et al. 2016) and the morphological evolution of tidal inlets (Velasquez-Montoya et al. 2020). Dredging activities around the Oregon Inlet area cost approximately five million dollars per year (North Carolina Coastal Federation 2016). Despite recent advancements in barrier island sediment transport modeling, data collection and better understanding of how soil properties affect erosion (Dolan et al. 2016; Safak et al. 2016), many questions remain unanswered. In particular, the evolution of Oregon Inlet has led to a dominant channel in the flood delta migrating toward the northern estuarine shoreline of Pea Island

(Velasquez-Montoya et al. 2020). This is hypothesized to accelerate erosion of the marsh in that area. A study of aerial imagery in this region from 2003 to 2019 showed that erosion rates along this stretch of estuarine shoreline reached 3-4 m/yr over that period (Dunn et al. 2019). Ongoing current research indicates that up to 2-3 m of erosion can occur in one storm event.

This study is part of the DUNEX pilot experiment carried out in October 2019. It aims to collect initial in-situ geotechnical and hydrodynamic data within the tidal inlet channel adjacent to the estuarine shoreline of Pea Island and correlate it to local sediment grain size distributions and hydrodynamic conditions to improve the understanding of the local erosional processes.

STUDY AREA

The survey area is located just south of Oregon Inlet (<1 km) (Figure 1), along the estuarine side of Pea Island. Hurricane Dorian made landfall on Hatteras Island (south of Pea Island) on September 6, 2019, about a month prior to the October survey of Pea Island. Just days after the survey, tropical storm Melissa impacted Pea Island. Elevated water levels from the storm surge during tropical storm Melissa were observed from October 10 to 13 at station 8652587 at the Oregon Inlet Marina (Figure 2), just north of the survey site (NOAA 2020).

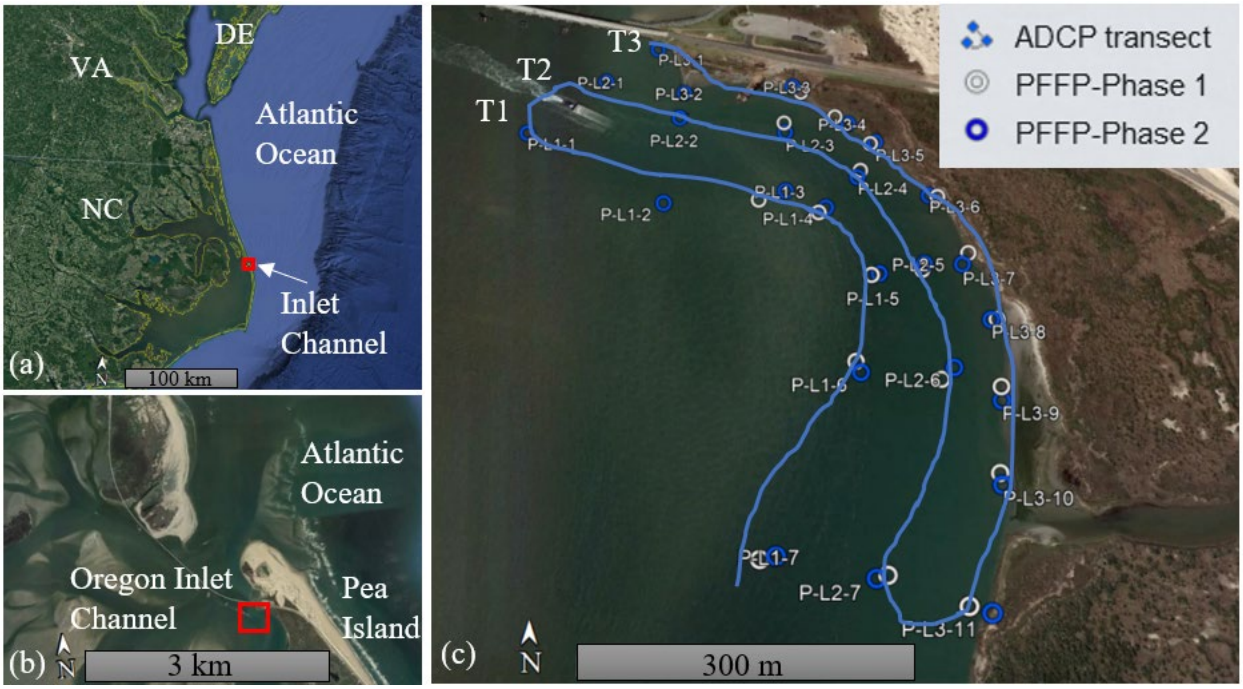

Figure 1. (a) Google Earth image of the Pea Island survey location (b) Zoomed image of the Oregon Inlet area (c) PFFP and ADCP transect measurements (Map data: Google, SIO, NOAA, U.S Navy, NGA, GEBCO).

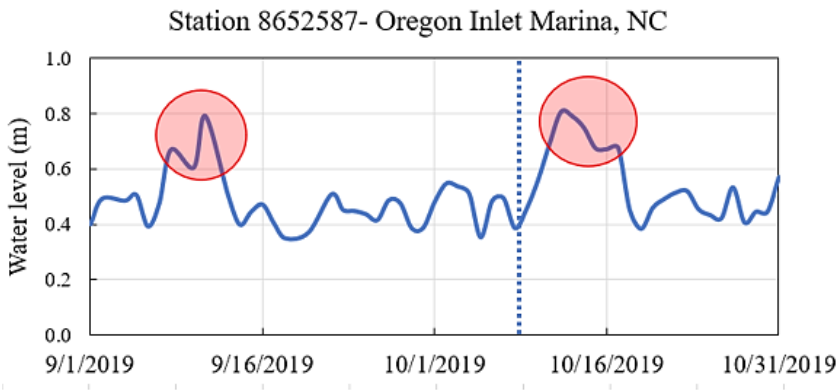

Figure 2. Water levels from the Oregon Inlet Marina, NC, Station 8652587 (NOAA 2020). The red circles show the surge in water levels from hurricane Dorian and tropical storm Melissa. Dashed line pertains to the date of measurements (Oct. 8th).

INVESTIGATION

A portable free fall penetrometer (PFFP), with a tapered body (~63 cm long) and conical tip was used in this survey. The PFFP was deployed in the southern most channel of Oregon Inlet along three transects with water depths ranging from less than 1 m up to 16 m. There was a total of 25 locations spread out over three transects with duplicate deployments at each location for validity. Surveys were conducted along the three transects during two different tidal current phases: phase 1 corresponding to early flood and phase 2 corresponding to near-max flood conditions (Figure 2). Sediment grab samples were also collected two days later at every deployment location for grain size analysis. The penetrometer free falls under self-weight through the water column and into the seabed. Five accelerometers record decelerations ranging from ± 2 *g* to ± 250 *g* (with *g* being the gravitational acceleration) at a rate of 2 kHz. The device penetrates the seabed until sediment resistance halts any further advancement. The first and second integration of the deceleration-time profiles yield the impact velocity and penetration depth, respectively. The sediment resistance force can be calculated from the PFFP deceleration rate using Newton's Second Law, assuming that all deceleration is a result of sediment resistance. Next, the dynamic bearing capacity, $q_{dyn,}$ can be calculated by dividing the sediment resistance by the area subject to loading. Finally, q_{dyn} is divided by a strain rate correction factor to estimate a quasi-static bearing capacity (*qsbc*) to account for the high impact velocity of the penetrometer (on the order of meters per second). No standard has been developed for PFFP survey strategies or data analysis. However, this study followed the example by Stark et al. (2012) that has been applied in many subsequent PFFP studies and is still being applied to-date, particularly at sites with limited previous knowledge of the local sediments.

A boat-mounted acoustic Doppler current profiler (ADCP) was used to measure the vertical current profiles near the penetrometer drop locations. Currents were recorded continuously and averaged every 10 seconds. An RTK-GPS was used to locate ADCP measurements and measure boat motions throughout the survey period by recording the boat's position every second. The ADCP was rigidly mounted facing downward with transducers roughly 0.1 m into the water. The blanking distance from the transducers was 0.2 m and velocities were recorded in 0.5 m cell increments. Raw velocities were converted to geographic coordinates, accounting for magnetic

declination. Velocity with amplitudes less than 55 dB and correlations less than 50% were omitted from the data.

To calculate the depth-averaged and depth-varying velocity at each drop location, velocity measurements within 10 meters of the drop position and within 10 minutes of the drop time were collected. Velocity measurements over depths greater or less than one standard deviation from the average depth within the penetrometer drop location were removed. A single depth-averaged velocity at the drop location was determined using a weighted average to account for the distance from the drop location.

Once the investigation was completed, variations in the estimated deceleration and *qsbc* profiles along the deployment locations with sediment properties and current velocities were evaluated to further understand the sediment dynamics in the vicinity of Oregon Inlet.

RESULTS AND DISCUSSION

The PFFP measurements were carried along three transects (T1, T2, T3) consisting of 25 total locations evenly spaced out over 1000 m within the Oregon Inlet channel. Six deployments out of 50 were omitted from the dataset due to irregular deceleration profiles. The impact velocity of the PFFP varied mostly between 5 and 6 m/s among all transects. Eight outliers lower than 5 m/s or higher than 6 m/s were observed mainly in phase 2 drops along transect 3, likely associated with shallow water depths and limited free fall. The results of the PFFP measurements, grain size analyses, and ADCP recordings are discussed for each transect.

Transect 1

As shown in Figure 1c, transect 1 (T1) was the furthest away from the shoreline. The maximum decelerations recorded for each drop ranged from 45 *g* to 75 *g* during phase 1, and from 45 *g* to 85 *g* during phase 2. The *qsbc* vs. depth profiles between the two deployment phases at each location exhibited very little variation overall. The maximum *qsbc* along the *qsbc*-depth profile was used for description and comparison among sites and referred to hereafter as *qsbc* only. The *qsbc* recorded during phase 1 of the survey had an average of 135 kPa, with the lowest *qsbc* of 75 kPa observed at PL1-7 and the highest *qsbc* of 140 kPa observed at PL1-3 (Figure 3). The *qsbc* results were reported at sediment depths between 4 and 6 cm, except for PL1-7 (at a depth of ~8.5 cm).

The profiles during phase 2 did not seem to vary significantly from phase 1, except at a few sites, including PL1-5 and PL1-6 (Figure 4). Two additional deployment locations were added to phase 2 of the survey (PL1-1 and PL1-2) up north. The average *qsbc* during phase 2 increased slightly to ~ 143 kPa with a similar lowest *qsbc* of 77 kPa but a higher *qsbc* of 330 kPa (Figure 3). The sediment depths associated with *qsbc* values during phase 2 generally matched the depths reported at phase 1.

Minor changes in *qsbc* results during phase 2 indicated an increase at sites PL1-6 and PL1-7, a decrease at sites PL1-3 and PL1-4, and slight variations at site PL1-5. The decrease in the *qsbc* reported at PL1-3 and PL1-4 was measured at deeper sediment depths, while an increase in *qsbc* reported at PL1-6 and PL1-7 was measured at shallower sediment depths. The sediments collected were classified as fine sands (USCS), and the average median grain size (d_{50}) decreased downstream from 350 μm at PL1-3 to 220 μm at PL1-7.

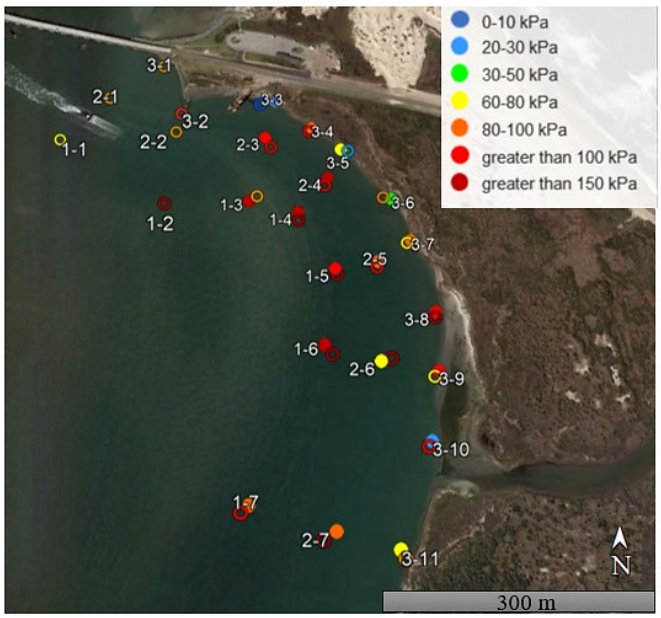

Figure 3. Maximum *qsbc* observed at each PFFP deployment location along all transects. Filled and non-filled circles represent results during phase 1 and 2 of the survey, respectively.

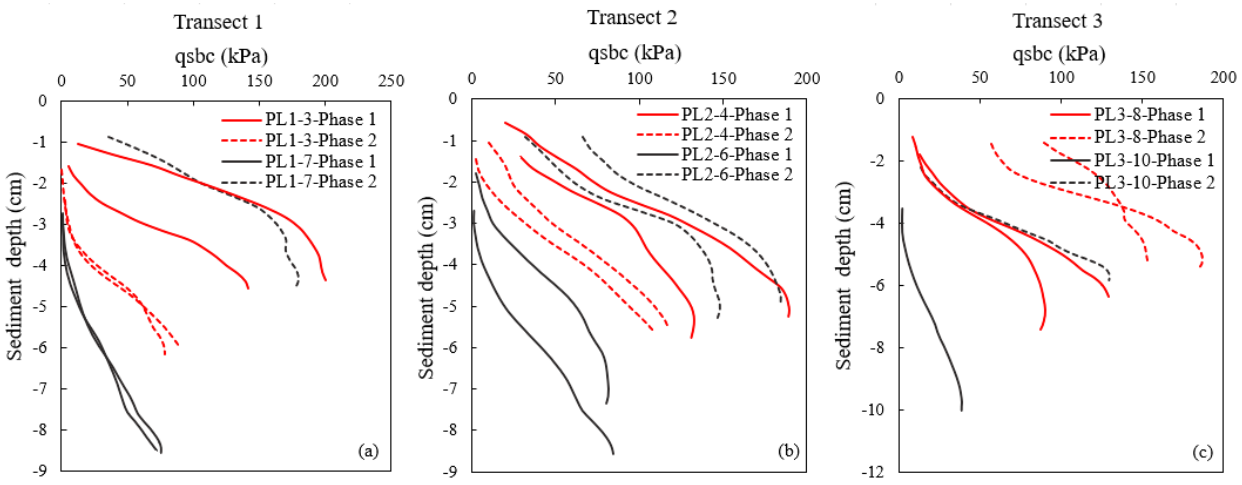

Figure 4. PFFP *qsbc*-depth profiles observed at (a) T1, (b) T2 and (c) T3. Solid and dashed black lines pertain to the two deployments surveyed during phase 1 and phase 2 of the survey, respectively and different colors pertain to the deployment location (locations with lowest and highest recorded *qsbc* values were selected).

A loose sediment top layer (LSTL), defined by low deceleration values (<1 *g*), was observed at some deployment locations during phase 1 of the survey. A LSTL usually indicates that sediments were deposited recently. Recent sediment deposition may be the result of localized sediment remobilization caused by changes in hydrodynamic conditions (Stark and Kopf 2011; Albatal and Stark 2017). Although the LSTL was relatively thin during phase 1 (not exceeding 3 cm of thickness), the LSTL thickness was negligible during phase 2 of the survey. This reduction

in LSTL thickness may be the result of the change in flood phase between phase 1 and 2, as was earlier suggested in literature (Albatal and Stark 2017).

Current velocities were measured using the ADCP (Figure 5) and processed as described earlier to yield one current magnitude value for each PFFP deployment location. Expectedly, the currents are higher during phase 2 of the survey (near-maximum flood stage), with an average value of 0.47 m/s across all locations, compared to a value 0.31 m/s during phase 1 (Figure 5). The highest current velocities were measured during phase 2 at locations PL1-1, PL1-6, PL1-7, with average velocities ~ 0.75 m/s. Thus, the reported increase in *qsbc* at PL1-6 and PL1-7 during phase 2 coincided with high flow velocities (Figure 5) and likely resulted from erosion of looser sand surface layers leaving a denser surface.

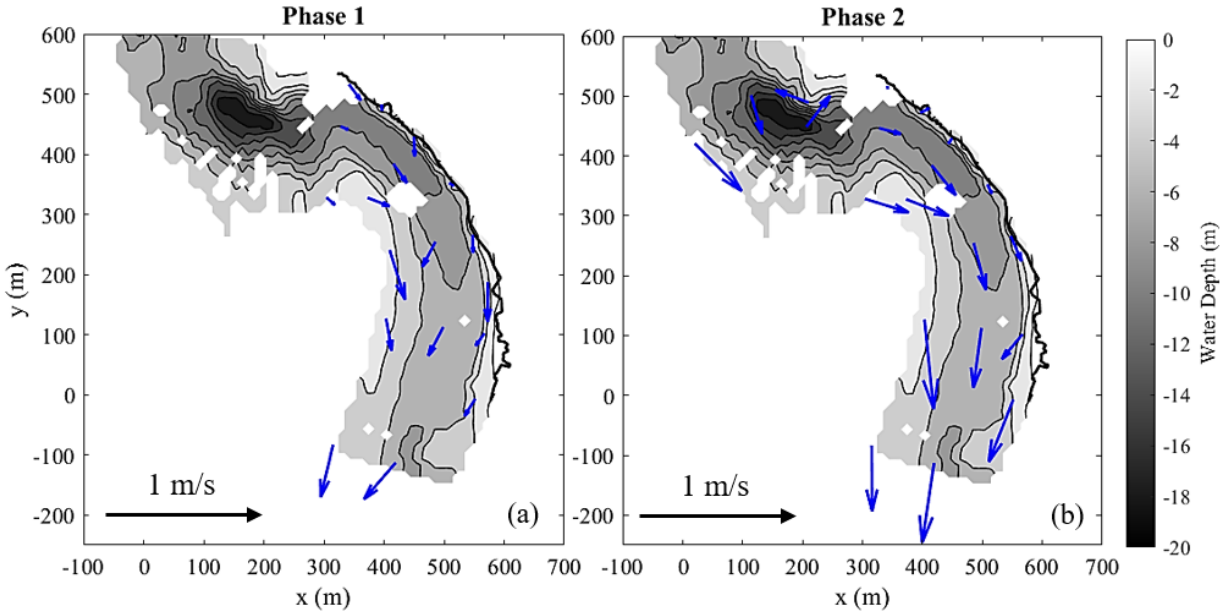

Figure 5. Measured current velocities at the PFFP deployment locations (Figure 1). Blue arrows represent the measured magnitudes during (a) phase 1 and (b) phase 2 of the survey. Reference point (0,0) is at 35°45'41.20''N and 75°31'44.98'' W.

Transect 2

Transect 2 (T2) is the middle transect between transects 1 and 3 and is closer to the channel shoreline than T1 (Figure 1). The deployments were overall consistent between phases 1 and 2. The average *qsbc* along T2 was ~ 101 kPa, with a lowest *qsbc* of ~65 kPa and a highest of ~190 kPa (Figure 3). PL2-3 and PL2-4 recorded the highest *qsbc* values along T2 compared to the sites downstream with the lowest *qsbc* values (PL2-5, PL2-6, and PL2-7). The *qsbc* values at upstream sites were measured at sediment depths of 5 to 6 cm, in contrast with the slightly deeper depths at downstream sites of 7 to 9 cm.

As the flood stage approached its peak, similar observations to T1 were noticed at T2 with respect to the changes in the *qsbc* values per deployment locations. The average *qsbc* along T2 increased to ~ 158 kPa, PL2-3 and PL2-4 (northward upstream sites) recorded a decrease in sediment strength, while PL2-6 and PL2-7 (downward downstream sites) reported an increase in *qsbc* values recorded at shallower depth. Similar to transect 1, PL2-5 measured almost no change

in the *qsbc*. Sediments along T2 were classified as fine sands, except for PL2-2 which had more than 50% fines and a mean grain size of 22 μm. The remaining d_{50} results showed an increase in grain size in the downstream direction from 190 μm at PL2-3 up to 313 μm at PL2-6.

The current velocities also increased in the downstream direction from PL2-3 to PL2-7, with higher values recorded during phase 2 of the survey. The highest recorded current velocities were observed at PL2-6, PL2-7 with 0.7 and 0.92 m/s during phase 2, respectively.

Transect 3

Transect 3 (T3) is located along the channel bank, as shown in Figure 1c. Trends in *qsbc* along T3 were somewhat similar to those observed at T1 and T2. Downstream sites PL3-10 and PL3-11 exhibited lower *qsbc* values than the upstream sites (Figure 3). However, a significantly lower *qsbc* value of approximately 7 kPa was recorded at a depth of approximately 30-42 cm at PL3-3, the phase 1 location farthest upstream and sheltered by a spit and a dock. This was the greatest penetration depth recorded among T3 deployments. Although no samples were retrieved at PL3-3, irregularities in the *qsbc*-depth profile obtained from PFFP results seemed to indicate muddy sediments, which was confirmed by site observations during the survey. Also, the average *qsbc* along T3 increases from 63 kPa to 84 kPa from phase 1 to phase 2 of the survey. However, the change in *qsbc* within T3 seems rather abrupt with no clear trend of increase or decrease in *qsbc* based on deployment locations (Figure 4). Nonetheless, sites PL3-8 up to PL3-11 showed either an increase or no change in *qsbc* compared to the upstream sites that showed either an increase or decrease at different sites.

The coarsest sediments were found at downstream sites (PL3-8-PL3-11) with a d_{50} varying from 230 μm to 300 μm. Lower d_{50} values were observed upstream between PL3-4 and PL3-7 ranging from 72 μm to 194 μm where lower *qsbc* results and thicker LSTL were observed. The highest *qsbc* values were observed at PL3-8 during both phase 1 and phase 2. The higher recorded *qsbc* was related to a low fines content at that location (<10% fines). Gradation tests of samples from PL3-5 revealed more than 50% fine sediments, with a d_{50} of 74 μm, which explained the low *qsbc* observed at this location.

The increase in current velocity magnitudes discussed in T1 and T2 during phase 2 was also observed here, but to a lesser extent, with the maximum velocity of 0.73 m/s recorded at PL3-10. In general, the current velocities observed along T3 were lower than velocities observed along T1 or T2, this is likely due to flow deceleration caused by bank and bottom friction as the currents enter shallower waters near the channel banks.

Transect Comparison

The variations in *qsbc* and sediment grain size recorded among and within each of the three transects appear related to the two phases of the flood current. The fine sands observed along T1 seem to be relatively strong (100-200 kPa) and mostly consistent throughout the transect. Weaker soils observed near the southern side of the transect, downstream of the channel, typically had a smaller grain size. As the tide approached the maximum flood stage, soil strength decreased at the upstream locations and increased at the downstream locations where also the higher current velocities were observed. The change in sediment strength, or maximum *qsbc*, was related to the change in sediment depth at which this *qsbc* is observed, where higher *qsbc's* were observed at

shallower sediment depths. This can be explained by the fact that stronger soils provide more resistance against the PFFP advancement resulting in a shallower penetration depth (Albatal et al. 2017). The trend of strength variations among locations was coupled with the more significant increase in current velocities observed at downstream locations during phase 2 of the survey. The increase in water velocities also resulted in a significant decrease in LSTL thickness. A similar trend in strength and current variations was observed along T2, but with lower *qsbc* values and slightly lower current velocities. However, approaching the shoreline towards T3, some of the trends were disrupted by the presence of significantly finer sediments in locations possibly more sheltered from the tidal current but where the marsh shoreline has been reported to be eroding at an average rate of 3 m/yr.

CONCLUSION

The results presented here suggest specific trends in soil properties based on locations and proximity to shorelines: stronger and more sandy sediments prevailed further away from the banks and inlet associated with stronger velocity magnitudes during flood currents. Significantly softer and finer sediments were located close to shore and where sheltered from the flood current. Based on the limited data collected along a short section of the shoreline, these conclusions promise that the combination of methods applied here facilitates important insights into local sediment dynamics in complex systems, like tidal inlet channels.

ACKNOWLEDGMENTS

The authors acknowledge the National Sciences Foundation for funding the research presented here through grant CMMI-1751463. Field deployments were conducted as part of the During Nearshore Event Experiment (DUNEX), which was facilitated by the U.S. Coastal Research Program (USCRP). We thank USCRP for their support of this effort through logistics and coordination. The authors also acknowledge comments by two anonymous reviewers that contributed to the improvement of the article.

REFERENCES

Albatal, A., and Stark, N. (2017). “Rapid sediment mapping and in situ geotechnical characterization in challenging aquatic areas.” *Limnology and Oceanography: Methods*, 15(8), 690-705.

ASTM D2487-11. Standard Practice for Classification of Soils for Engineering Purposes (Unified Soil Classification System). *ASTM International*, West Conshohocken, PA.

Clinch, A. S., Russ, E. R., Oliver, R. C., Mitasova, H., and Overton, M. F. (2012). “Hurricane Irene and the Pea Island Breach: Pre-storm Site Characterization and Storm Surge Estimation Using Geospatial Technologies.” *Shore and Beach*, 80(2), 38–46.

Dayal, U., & Allen, J. H. (1973). “Instrumented Impact Cone Penetrometer.” *Canadian Geotechnical Journal*,10(3), 397-409.

Dolan, R., & Lins, H. F. (2000). “The Outer Banks of North Carolina.” *US Geological Survey,* Professional Paper, 1177-B, 58-110.

Dolan, R., Lins, H.F., and Smith, J.J., (2016). “The Outer Banks of North Carolina.” *U.S. Geological Survey*, Professional Paper, 1827,153-289.

Dunn, M., Sciaudone, E., and Velasquez-Montoya, L. (2019) "Estuarine shoreline erosion driven by flood channel proximity at Pea Island, NC." Proc. American Shore & Beach Preservation Association (ASBPA) National Coastal Conference 2019, Myrtle Beach, SC.

Grabowski, R. C., Droppo, I. G., & Wharton, G. (2011). "Erodibility of cohesive sediment: The importance of sediment properties." *Earth-Science Reviews*, *105*(3-4), 101-120.

Inman, D. L., & Dolan, R. (1989). "The Outer Banks of North Carolina: Budget of sediment and inlet dynamics along a migrating barrier system." *J. of Coastal Research*, 193-237.

NOAA (National Oceanic and Atmospheric Administration) (2019). "USGS current conditions for the nation-station 08114000." < https://nwis.waterdata.usgs.gov/nwis/uv?> (August 25, 2019).

North Carolina Coastal Federation (2016) "North Carolina's terminal groins at Oregon Inlet and Fort Macon". North Carolina Coastal Federation.< https://www.nccoast.org> (August 20,2020).

Overton, M., (2015). "Coastal monitoring program, NC 12 transportation management plan, TIP project B-2500, 2014 Update Report." *Final report prepared for NCDOT*.

Pietrafesa, L. J. (2012). "On the continued cost of upkeep related to groins and jetties." *J. of Coastal Research*, 28(5), 3-4.

Riggs, S. R., & Ames, D. V. (2009). "Impact of the oregon inlet terminal groin on downstream beaches of Pea Island, NC Outer Banks." *White Paper for NC Division of Coastal Management.*

Riggs, S. R., Ames, D. V., Culver, S. J., Mallinson, D. J., Corbett, D. R., & Walsh, J. P. (2009). "Eye of a human hurricane: Pea island, Oregon inlet, and bodie island, northern outer banks, North Carolina." *Geological Society of America Special Papers*, 460(4), 43-72.

Safak, I., J. C. Warner, and J. H. List (2016). "Barrier island breach evolution: alongshore transport and bay-ocean pressure gradient interactions." *J. Geophys. Res. Oceans*, 121, 8720– 8730.

Sciaudone, E. J., Velasquez-Montoya, L., Smyre, E. A., & Overton, M. F. (2016). "Spatial and temporal variability in dune field: Pea Island, North Carolina." *Shore & Beach*, 84(2), 49-58.

Seminack, C.T., and McBride, R. A. (2018). "A life cycle model for wave dominated tidal inlets along passive margin coasts of North America." *Geomorphology*, 304, 141-158.

Stark, N., and Wever, T.F. (2009). "Unraveling subtle details of expendable bottom penetrometer (XBP) deceleration profiles." *Geo-Marine Letters*, 29(1), 39–45.

Stark, N., and Kopf, A. (2011). "Detection and quantification of sediment remobilization processes using a dynamic penetrometer." Proc. IEEE/MTS Oceans 2011, Waikoloa, HI.

Velasquez-Montoya, L. V., Sciaudone, E. J., Mitasova, H., & Overton, M. F. (2018)." Observation and modeling of the evolution of an ephemeral storm-induced inlet: Pea Island Breach, North Carolina, USA." *Continental Shelf Research*, 156, 55-69.

Velasquez-Montoya, L., Overton, M. F., & Sciaudone, E. J. (2020). "Natural and anthropogenic-induced changes in a tidal inlet: Morphological evolution of Oregon Inlet." *Geomorphology*, 350(1),106871.

Velasquez-Montoya, L., Sciaudone, E.J., Smyre, E., and Overton, M. F. Forthcoming. "Vulnerability indicators for coastal roadways based on barrier island morphology and shoreline change predictions." *Natural Hazards Review*.10.1061/(ASCE)NH.1527-6996.0000441.